J. Anat. (2006) **208**, pp13–19

Calcium phosphate microcrystal deposition in the human intervertebral disc

Robert S. Lee, Mike V. Kayser and S. Yousuf Ali

Institute of Orthopaedics, Royal National Orthopaedic Hospital, Stanmore, Middlesex, UK

Abstract

A variety of crystals have been identified in both normal and pathological connective tissues. Calcium phosphate 'cuboidal' microcrystal deposition has been found, using transmission electron microscopy (TEM), in femoral articular cartilage, where they are distributed as a band 5–50 μm beneath the articular surface. These cuboid microcrystals have been identified as magnesium whitlockite. Our objective was to investigate their presence in the human intervertebral disc. In this study, two degenerate and 15 scoliotic discs were examined using light microscopy and TEM techniques to determine the presence of calcium phosphate crystals. Calcium pyrophosphate dihydrate (CPPD) deposition was identified in one degenerate disc specimen. Using TEM and electron probe analysis, cuboid microcrystals were identified in the annulus fibrosus and nucleus pulposus of both degenerate specimens, but not in the discs from young scoliotic patients. Cuboid microcrystal deposition was found predominantly around cells, which were mainly necrotic, with some association with extracellular lipidic/membranous debris. This is the first TEM report of whitlockite in the intervertebral disc. In one specimen coexistence of cuboid and CPPD crystal deposition was found.

Key words calcium pyrophosphate dihydrate; crystal deposition disease; disc degeneration; magnesium whitlockite.

Introduction

The involvement of crystals in joint disease is a relatively new concept in historical terms and has led to the use of the term 'crystal deposition disease'. Many types of crystals have been identified in joints and, in some cases, their role in the consequent pathology has been determined (McCarty, 1994). 'Cuboid crystals', characterized as magnesium whitlockite, have been found in various sites including normal and osteoarthritic femoral cartilage (Ali & Griffiths, 1981; Ali, 1985; Ali et al. 1992; Scotchford et al. 1992) and in the meniscus and articular cartilage of the knee (Dunbar Rees, 1995). These crystals are too small to be resolved by light microscopy or radiographically.

'Cuboid' calcium phosphate crystals were first identified by Ali & Griffiths (1981) in arthritic femoral head cartilage and since then in many other independent studies (Ghadially & Lalonde, 1981; Scotchford & Ali, 1982; Marante et al. 1983; Rees et al. 1986; Stockwell, 1990; Ali & Scotchford, 1992; Ali et al. 1992; Scotchford et al. 1992; Bardin et al. 1993). These crystals appear as a band up to 50 μm beneath the cartilage surface, with their size varying from 50 to 200 nm. Electron probe analysis showed that their calcium/phosphate (Ca/P) ratio was lower than that of hydroxyapatite (HAP). Scanning electron microscopy has shown that these crystals are indeed cuboid, or to be precise, rhombohedral in shape. The presence of a small amount of magnesium with the calcium and phosphorus is indicative of whitlockite. Although these crystals were identified in osteoarthritic cartilage, they have also been seen in normal cartilage with a smooth articular surface though no difference in Ca/P ratio of crystals from normal and osteoarthritic specimens has been observed. The crystals were on one occasion observed to be adjacent to pyrophosphate crystals, suggesting mixed crystal deposition (Ali, 1985). The cuboid crystals have also been observed in close association with lipidic or vesicular membranous debris.

Correspondence
Mr Robert Lee BSc MBBS MRCS, Flat 4 Monterey Lodge, Frithwood Avenue, Northwood, Middlesex, HA6 3GA, UK. T: +44 (0)7958 443326; F: +44 (0)1923 841655; E: leerobert9@hotmail.com

Accepted for publication *7 October 2005*

Pathological calcification of the disc was first described by Luschka (1855), who observed chalk-like deposits in disc tissue at autopsy, and later elaborated by Calvé & Galland (1930). There have since been numerous reports of the presence of crystals in the disc, including calcium pyrophosphate (Pritzker, 1977) and HAP (Taylor & Little, 1963). The presence of deposits has been reported in association with some cases of thoracic disc prolapse, where it appears that there may initially be necrosis of the nucleus followed by subsequent calcification (Taylor et al. 1980). A previous study (Feinberg et al. 1990) showed that HAP, but not calcium pyrophosphate dihydrate (CPPD) deposits, were generally associated with histological signs of disc degeneration. Whether degeneration initiated crystal deposition or vice versa still remains a focus of debate. Calcification in association with scoliosis has also been reported (Roberts et al. 1993).

In degeneration of the disc, there is a substantial loss and degradation of proteoglycan in the nucleus pulposus (Lyons et al. 1981) with an accumulation of lipofuscin and lipidic debris (Ishii et al. 1991). Several mechanisms for this have been suggested, which include age (cell senescence), nutritional deficiency, spinal abnormality, mechanical influences resulting in fatigue failure of the matrix, immunological factors and post-translational modification of extracellular matrix components (Buckwalter, 1995).

Thus, whilst pathological calcification deposits of CPPD and HAP in the disc have been described, the presence of 'cuboid crystals' in the disc has not been reported to date, nor has an association be made between these crystals and degeneration of the disc or scoliosis.

Materials and methods

Specimens

Seventeen specimens of intervertebral disc were obtained during surgery from a total of five patients. Two of the discs were obtained from two patients with degenerate discs (aged 68 and 70 years; discs from level L4), presenting with spondylolisthesis, whilst the other 15 discs were from three scoliotic patients (aged 10, 12 and 20 years; T10 to L3, T11 to L1, T6 to T11, respectively), who underwent anterior release. Due to the procedure of surgical removal, the specimens were not obtained whole – they were resected as small 'nuggets' of tissue. As a result it was not possible to orientate the tissue. Thus, division of the tissue could only be made into annulus fibrosus and nucleus pulposus.

In all cases, the tissue was obtained within the first 5 min of resection. The tissue was collected and stored in a solution of 1.5% glutaraldehyde in 0.085 M sodium cacodylate buffer (pH 7.4). Random 'nuggets' of tissue were selected and processed for both light microscopy and electron microscopy.

Light microscopy (LM) processing

Slices of tissue were cut from the randomly selected nuggets of intervertebral disc. These were fixed for a minimum of 24 h in 10% formal saline and then processed through alcohol (90%, 100%), chloroform and wax, in a Reichert automatic tissue processor before embedding in wax. Two histological sections were cut from each block, each 5 μm in thickness, on a Leitz base sledge microtome and placed in an oven at 60 °C for a minimum of 1 h. Sections were dewaxed with xylene and rehydrated through a decreasing alcohol series. One section underwent staining with Harris's haematoxylin and eosin (H&E), whereas the other was stained with Weigert's haematoxylin, Alcian blue (0.5%) and Sirius Red (0.1%). All sections were examined and photographed with an Olympus BH2 photomicroscope.

Transmission electron microscopy processing

Samples of tissue from the annulus and nucleus pulposus were retreived, from which 1-mm square blocks were cut. These blocks then underwent standard fixation, dehydration and resin embedding processing exactly as described by Scotchford & Ali (1992). The tissue blocks were fixed in a solution of 1.5% glutaraldehyde in 0.085 M sodium cacodylate buffer (pH 7.4). Half the tissue blocks were then fixed with 1% osmium tetroxide. Following dehydration, the blocks were then transferred to propylene oxide prior to infiltration with 1 : 1 propylene oxide/araldite CY212 resin and then pure CY212 resin under vacuum overnight, before final embedding in fresh resin at 60 °C for 48 h.

Semithin (500 nm) and ultrathin (80–100 nm) sections were cut on a Reichert Ultracut E ultramicrotome. The semithin sections were stained with 1% toluidine blue in 1% borax. Ultrathin sections were cut with diamond knives and floated onto distilled water (pH 7.4), prior to collection onto G200 HS copper grids, which were precoated with 0.5% Formvar in chloroform.

The majority of specimens were observed unstained although, when required, the sections were stained with alcoholic saturated uranyl acetate, followed by Reynold's lead citrate.

The ultrathin sections were examined using a Philips CM12 transmission electron microscope operating at 80 kV. For the purposes of crystal identification, electron probe analysis was carried out on non-osmicated sections in order to determine the elemental composition of the crystals/particles seen.

Electron probe X-ray microanalysis

Spectra were recorded at 100 kV for 200 live seconds with a tilt angle of 20°, giving a total 'take-off angle' of 40°. A 70-nm 'top hat' condenser aperture was used to reduce the background effect. Ca/ P ratios were calculated using quantitative analysis of the thin sections software package (EDAX PV9800) based on the ratio model. Synthetic hydroxyapatite ($Ca_5(PO_4)_3OH$), tricalcium phosphate ($Ca_3(PO_4)_2$) and calcium pyrophosphate dihydrate ($Ca_2P_2O_7$), fixed and processed in the same way as the tissue specimens, were used as the calcium phosphate standards for these analyses. Ten spectra were taken for each calcium phosphate standard in the respective sections and each set was averaged to give the standards.

In total, 17 intervertebral discs were examined, with samples from both annulus and nucleus where possible. In all, 34 pieces of tissue were chosen and six blocks from each were processed, resulting in 204 resin blocks (half osmicated, half non-osmicated). Of these blocks 136 were examined (two osmicated and two non-osmicated) and a total number of 272 ultrathin sections were cut and examined.

Results

No radiographic evidence of calcification was observed in any of the patients. Macroscopically, the degenerate discs were extremely fragile and fibrous and showed browny discoloration. By contrast, the scoliotic specimens appeared in good condition with the nucleus pulposus having a gelatinous appearance.

Histological analysis

Light microscopic examination of scoliotic intervertebral discs revealed the typical histological appearance of well-organized tissue, with the annular lamellae clearly seen merging into the nucleus pulposus through the transition zone. Sections stained with Weigert's, Alcian blue and Sirius Red allowed greater differentiation between the structures. Alcian blue stains proteoglycans specifically, whereas the Sirius Red binds to collagen types I, II and III. Clear demarcation between the annulus and nucleus could be made solely on the basis of the red-stained annulus and blue-stained nucleus. The latter stain also imparts enhanced bifringency to the tissue because the dye aligns parallel to the collagen fibres (Junqueira et al. 1979) and thus examination under polarizing light clearly showed the different orientation of the collagen fibres in the adjacent lamellae.

Histological examination of the sections from degenerate discs showed marked contrast to the scoliotic discs. Atypical clumps of chondrocytes (chondrons) were observed, particularly in fibrillated areas. There was greater cellularity, with chondrocyte pairs sharing the same lacunae, as well as clusters of chondrocytes scattered throughout the irregular fibrous matrix. The sections stained a deeper colour than the scoliotic samples and staining with Weigert's, Alcian blue and Sirius Red, showing a lack of proteoglycan in the nucleus compared with the scoliotic nucleus. In addition, areas of the annulus and end-plate cartilage, staining yellow, were observed owing to lack of stain uptake by some of the collagen fibres. This may indicate structural changes in the collagen fibres in the degenerate disc. Small blood vessels were frequently observed penetrating into the degenerate disc.

In one patient, focal deposits of CPPD in both annulus and nucleus could be observed at the light microscope level. They appeared to be clearly demarcated focal clusters, with the crystals demonstrating weak positive bifringence. The crystals stained red–purple with H&E, whilst the Sirius Red stain imparted greater contrast, staining the crystals blue. There were also scattered crystal deposits in the vicinity of the main deposits.

No evidence of cuboid crystal deposition could be seen at the light microscope level.

TEM observations

Examination of the unstained ultrathin sections by TEM showed crystals in sharp contrast to the surrounding tissue in the degenerate disc specimens (Fig. 1), but not in the scoliotic specimens. The cuboid crystals were

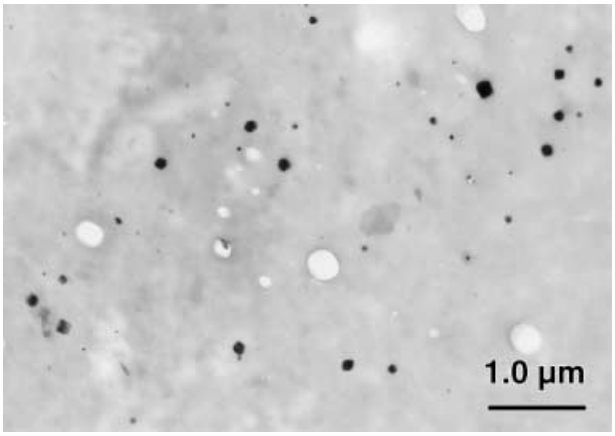

Fig. 1 Section of the nucleus pulposus of a degenerate intervertebral disc specimen (age 70 years, level L4), which demonstrates the typical size and morphology of the cuboid magnesium whitlockite crystals (unstained section).

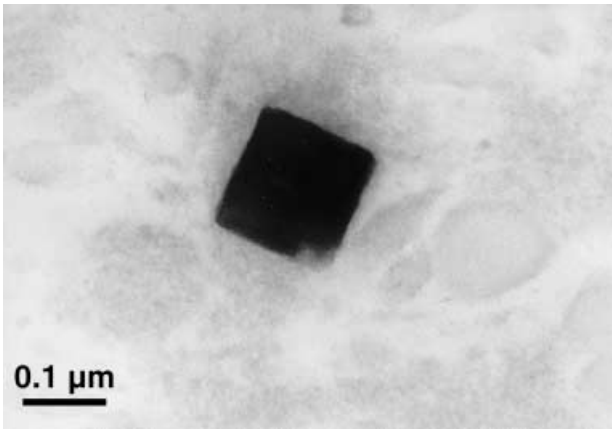

Fig. 2 High-magnification view of a typical cuboid crystal in the annulus fibrosus of a degenerate disc (unstained, osmicated specimen).

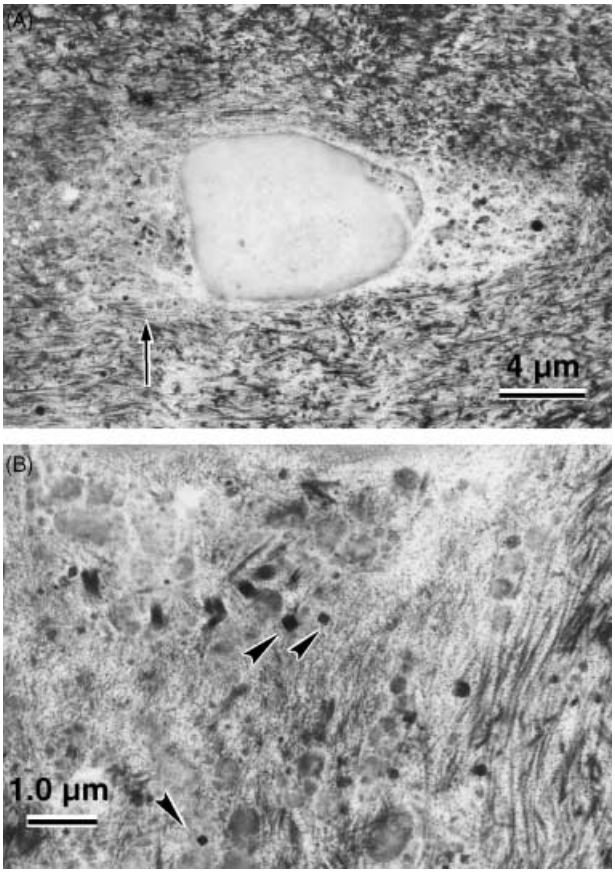

Fig. 3 (A) Cuboid crystals in the lacuna of a necrotic chondrocyte in the annulus fibrosus of a degenerate disc (stained with alcoholic uranyl acetate and lead citrate). (B) Magnification of the area indicated in (a; arrow), showing the association of the crystals (arrowheads) with cellular debris and membranous/vesicular bodies.

observed in both the annulus fibrosus and the nucleus pulposus of the degenerate intervertebral disc. They varied in size from 10 to 280 nm (Fig. 2). No association with any membrane around the cuboidal structure could be demonstrated. The crystals appeared to be predominantly distributed in the pericellular matrix or in association with necrotic chondrocytes (Fig. 3), although interterritorial distribution was also seen. Many of the cells in the degenerate disc appeared necrotic with extensive granular and amorphous debris surrounding the chondrocyte. Thus, the majority of cuboid crystals were observed in association with these membranous and vesicular bodies. There were no crystals seen in the intact (healthy) chondrocytes themselves, although they were observed in the lacuna of the chondrocytes. The crystal deposits were not abundant in distribution as compared with in the femoral articular cartilage (Scotchford & Ali, 1992), although local collections of crystals were observed as described above. This may be due to the relative acellularity of the tissue.

The CPPD crystals appeared rod like in longitudinal section and rhomboid in cross-section, but there was much variation in shape and size (Fig. 4). The deposits showed a typical 'brick-wall' formation. The crystals had a characteristic foamy appearance, with a substantial amount of sublimation under the electron beam due to loss of their water of crystallization. They ranged in length from 0.1 to 3.5 μm. In some sections, the deposits could be seen adjacent to red blood cells (Fig. 4). Although this was not a blood vessel, it resembled a vascular channel that had been created via a fissure in the disc tissue. On some occasions, CPPD crystals were

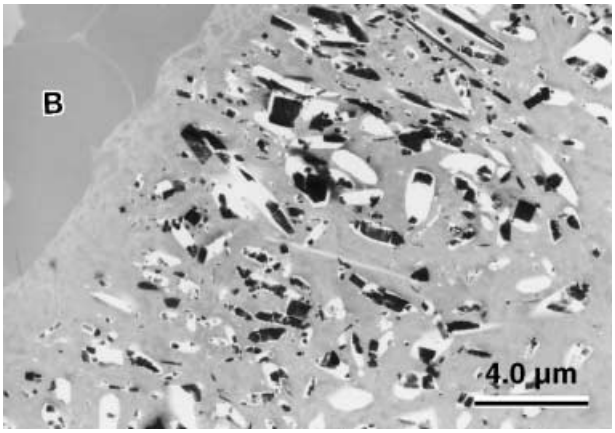

Fig. 4 Nucleus pulposus of a degenerate disc specimen showing a CPPD deposit, revealing the variety of crystal shape, rhomboid in cross-section and rod-shaped. Holes indicate areas of crystal dropout. Red blood cells (B) are seen in the adjacent vascular channel (unstained, osmicated section).

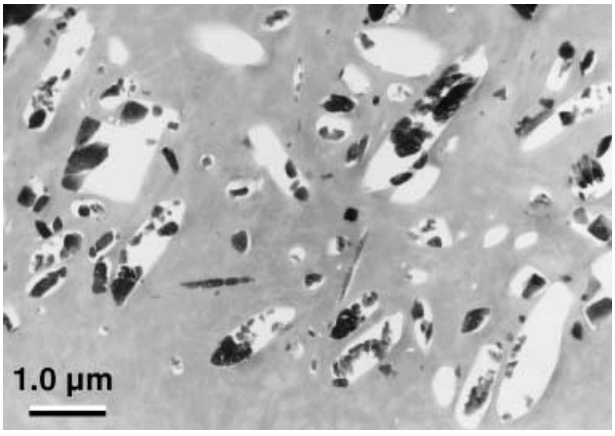

Fig. 5 Nucleus pulposus of a degenerate disc specimen showing coexistence of a CPPD deposit and a cuboid crystal. Electron probe analysis of the cuboid crystal gave a spectrum similar to that of magnesium whitlockite and other cuboid crystals (unstained, osmicated section).

observed in the necrotic chondrocytes themselves, although not in any intact (functional) chondrocytes. No specific association with collagen fibres was observed.

Cuboid crystals were seen in both degenerate discs, with coexistence of CPPD seen in one disc (Fig. 5).

Electron probe analysis

All crystals found were examined and their spectra analysed. The standards gave Ca/P ratios that were very close to their expected molar ratios. The Ca/P ratios of the standards and the resultant calibration line is shown in Fig. 6. The cuboid crystals that were observed

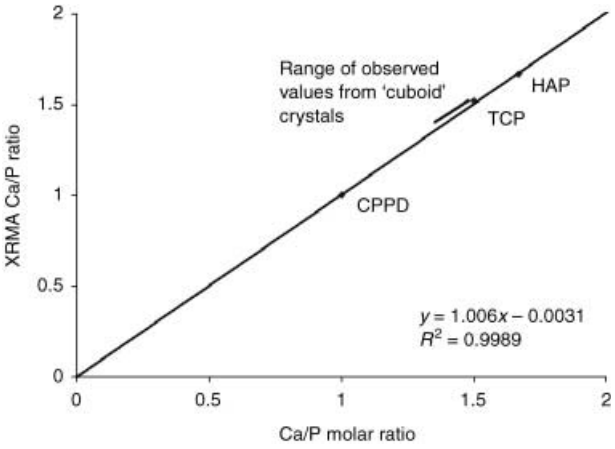

Fig. 6 Ca/P ratios for the standard calcium phosphate minerals observed by X-ray microanalysis (XRMA). The calibration curve shows the observed XRMA ratios plotted against the known Ca/P ratios. There is excellent correlation, the observed Ca/P ratios being 1.665 (SD = ±0.063), 1.519 (± 0.048) and 1.000 (± 0.009) for HAP, TCP and CPPD, respectively, compared with the expected molar ratios of 1.67, 1.50 and 1.00 (HAP = hydroxyapatite; TCP = tricalcium phosphate; CPPD = calcium pyrophosphate dihydrate).

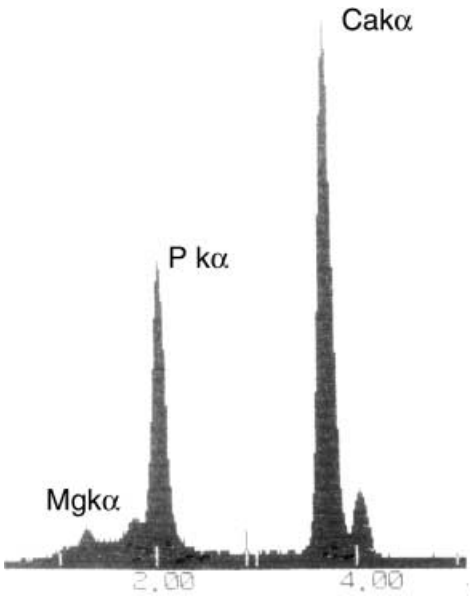

Fig. 7 Detail of the X-ray microanalysis spectrum generated by a cuboid crystal in the annulus fibrosus of a degenerate disc. Note the small magnesium peak (Kα at 1.25 keV).

in the degenerate discs gave spectra typical of whitlockite as reported by previous studies (Scotchford & Ali, 1992), an example of which is shown in Fig. 7. The major peaks corresponded to calcium (Kα at 3.69 keV) and phosphorus (Kα at 2.01 keV). A small magnesium peak was consistently observed (Kα at 1.25 keV).

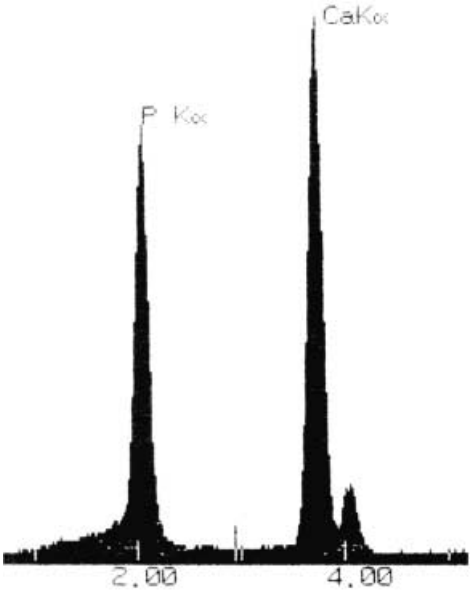

Fig. 8 Typical X-ray microanalysis spectrum generated by a CPPD crystal in the nucleus pulposus of a degenerate disc.

Because the specimens were collected in pH-adjusted distilled water, and not sodium cacodylate buffer (as carried out by Scotchford & Ali, 1992), any interference from an arsenic peak (Lα at 1.28 keV) was removed. The Ca/P ratio for the cuboid crystals ranged from 1.413 to 1.433. The CPPD crystals from one degenerate specimen gave a characteristic spectrum (Fig. 8) with major peaks corresponding to calcium and phosphorus. The average Ca/P ratio was calculated to be 1.021, again very close to the expected ratio of 1.00.

Discussion

This is the first study to report the presence of 'cuboid' magnesium whitlockite crystals in the degenerate intervertebral disc. Magnesium whitlockite was originally described as a geological mineral by Frondel (1941) and since then has been identified in a number of biological sites, usually in pathological situations, including dental calculi (LeGeros et al. 1988), urinary calculi (Santos & Gonzalez-Diaz, 1980), sialoliths (Burstein et al. 1979; Mishima et al. 1992), rhinoliths (Kodaka et al. 1994), aortic valvular tophi (Gawoski et al. 1985), appendix and mesentery nodes, nasal septum cartilage, tracheal cartilage, epiglottis (Rowles, 1968), calcified abdominal aorta (Reid & Andersen, 1993), pulmonary nodules (Pritzker & Luk, 1976), as well as in the synovial fluid of patients with 'Milwaukee shoulder' syndrome (McCarty et al. 1983). The detection of these crystals by TEM has been well documented in femoral head articular cartilage, where they form a band 5–50 μm beneath the articular surface. The size of the crystals found in this study (10–200 nm) correlates well with previous reports by Scotchford & Ali (1995), who described a size range of 50–500 nm. Apart from this study there has only been one other report of their presence in the intervertebral disc (Rowles, 1968), where the crystals were isolated for the purpose of molecular characterization by X-ray diffraction. There was, however, no description of whether the specimens were normal, aged, degenerate or scoliotic.

The possibility that these cuboid crystals may simply be an artefact of processing has been ruled out by all the previous studies from various laboratories and by a comprehensive study by Scotchford et al. (1995). Previous studies showed no artefactual displacement of crystals during tissue preparation (Rees et al. 1986) and equally supportive evidence is their absence in the discs from scoliotic patients and from epiphyseal cartilage (Scotchford & Ali, 1995), using exactly the same technique.

Care must be taken when interpreting the absence of these crystals in the scoliotic specimens as the small sample number, lack of male specimens and lack of older samples precludes any definite conclusions. Nevertheless, this study can act as a preliminary investigation on which further research can be based.

The crystals observed in this study bore great similarity to cuboid crystals previously described, in terms of size, shape and observed Ca/P ratio. There was no significant difference between the Ca/P ratios for the cuboid crystals found in the nucleus and annulus, suggesting that the crystals in both sites are chemically similar. Nor was there any correlation between crystal size and Ca/P ratio as was previously suggested (Rees et al. 1986).

The location of these crystals in the intervertebral disc is similar to that in articular cartilage, being present in the pericellular matrix and with membranous/vesicular bodies, particularly so around areas of chondrocyte necrosis. Ghadially & Lalonde (1981) used the term 'intramatrical debris' to describe the pericellular lipid, which is probably derived from the cytoplasmic processes of chondrocytes. They noted a close association between what they termed 'calcified bodies' (which resembled the cuboid crystals) and this intramatrical debris in the human meniscus. A similar association between magnesium whitlockite and lipidic debris has been shown by Scotchford & Ali (1995) and in aging cartilage (Marante et al. 1983).

Cuboid crystal deposition has thus been observed in both the annulus fibrosus and the nucleus pulposus of both degenerate disc specimens, but not in the scoliotic specimens. Electron probe analysis confirmed the identity of the crystals to be magnesium whitlockite, similar to previous reports of whitlockite crystal deposition in articular cartilage. Whether these crystals may be involved in the process of disc degeneration or arise as a result of the pathological process is yet to be determined.

References

Ali SY, Griffiths S (1981) New types of calcium phosphate crystals in osteoarthritic cartilage. *Sem Arthritis Rheum* **11** (Suppl. 1), 124–126.

Ali SY (1985) Apatite type crystal deposition in arthritic cartilage. *Scann Electron Microsc* **4**, 1555–1666.

Ali SY, Rees JA, Scotchford CA (1992) Microcrystal deposition in cartilage and osteoarthritis. *Bone Miner* **17**, 115–118.

Ali SY, Scotchford C (1992) Electron microscopy and X ray analysis of calcium phosphate microcrystals in human articular cartilage. In *Electron Microscopy, 3. EUREM, Granada, Spain*, pp. 633–634.

Bardin T, Lansaman J, Bucki B, et al. (1993) Tricalcium phosphate crystal identification in human cartilage. An ultrastructural and elemental analysis. *Arth Rhem* **35**, S161.

Buckwalter JA (1995) Aging and degeneration of the human intervertebral disc. *Spine* **20**, 1307–1314.

Burstein LS, Boskey AL, Tannerbaum PJ, Posner AS, Mandel IR (1979) The crystal chemistry of submandibular and parotid salivary gland stones. *J Oral Pathol* **8**, 284–291.

Calvé J, Galland M (1930) The intervertebral nucleus pulposus, its anatomy, its physiology, its pathology. *J Bone Joint Surg* **12**, 555–578.

Dunbar Rees R (1995) *Presence of Mg whitlockite crystals in knee articular cartilage of patients with osteoarthritis*. BSc research project, University of London, Institute of Orthopaedics, RNOHT, Stanmore.

Feinberg J, Boachie Adjei O, Bullough PG, Boskey AL (1990) The distribution of calcific deposits in the intervertebral discs of the lumbosacral spine. *Clin Orth Rel Res* **254**, 303–310.

Frondel C (1941) Whitlockite a new calcium phosphate, $Ca_3(PO_4)_2$. *Am Miner* **26**, 145–152.

Gawoski JM, Balogh K, Landis WJ (1985) Aortic valvular tophus, identification by X ray diffraction of urate and calcium phosphates. *J Clin Pathol* **38**, 873–876.

Ghadially FN, Lalonde JMA (1981) Intramatrical lipidic debris and calcified bodies in human semilunar cartilages. *J Anat* **132**, 481–490.

Ishii H, Sano A, Katoh Y, Matsui H, Terahate N (1991) Histochemical and ultrastructural observations on brown degeneration of human intervertebral disc. *J Orthop Res* **9**, 78–90.

Junqueira LCU, Bignolas G, Brentani RR (1979) Picrosirius staining plus polarization microscopy, a specific method for collagen detection in tissue sections. *Histochem J* **11**, 447–455.

Kodaka T, Debari K, Sano T, Yamada M (1994) Scanning electron microscopy and energy dispersive X ray microanalysis studies of several calculi containing calcium phosphate crystals. *Scan Microsc* **8**, 241–257.

LeGeros RX, Orly I, Legeros JP, et al. (1988) Scanning electron microscopy and electron probe microanalyses of the crystalline components of human and dental calculi. *Scan Microsc* **2**, 345–356.

Luschka H (1855) Die Altersveranderungen der Zwischenwirbelknorpel. *Arch Path Anat* **IX**, 311–327.

Lyons G, Eisenstein S, Sweet K (1981) Biochemical changes in intervertebral disc degeneration. *Biochim Biophys Acta* **673**, 443–453.

Marante I, Macdougall AR, Stockwell RA (1983) Ultrastructural observations of crystals in articular cartilage of aged human hip joints. *Ann Rheum Dis* **42** (Suppl.), 96–97.

McCarty DJ, Lehr JR, Halverson PB (1983) Crystal populations in human synovial fluid. *Arth Rheum* **26**, 1220–1224.

McCarty DJ (1994) Crystals and arthritis. *Dis A Month* **40**, 253–299.

Mishima H, Yamamoto H, Sakae T (1992) Scanning electron microscopy energy dispersive spectroscopy and X ray analyses of human salivary stones. *Scan Microsc* **6**, 487–494.

Pritzker KPH, Luk SC (1976) Apatite associated arthropathies, preliminary ultrastructural studies. *Scan Electron Microsc* **III**, 493–499.

Pritzker KPH (1977) Aging and degeneration in the lumbar intervertebral disc. *Orth Clin North Am* **8**, 65–77.

Rees JA, Ali SY, Mason AZ (1986) Scanning electron microscopy and microanalysis of 'cuboid' crystals in human articular cartilage. In *Cell Mediated Calcification and Matrix Vesicles* (ed. Ali SY), pp. 365–371. Amsterdam: Elsevier.

Reid JD, Andersen ME (1993) Medial calcification (whitlockite) in the aorta. *Atherosclerosis* **101**, 213–224.

Roberts S, Menage J, Eisenstein SM (1993) The cartilage end plate and intervertebral disc in scoliosis, calcification and other sequelae. *J Orth Res* **11**, 747–757.

Rowles SL (1968) The precipitation of whitlockite from aqueous solution. *Bull Soc Chimie France* 1797–1802.

Santos M, Gonzalez-Diaz PF (1980) Ultrastructural study of apatites in human urinary calculi. *Calcif Tiss Int* **31**, 93–108.

Scotchford C, Ali SY (1992) Calcium phosphate microcrystal deposition in articular cartilage, characterization by XRMA. *Micron Microsc Acta* **23**, 383–384.

Scotchford CA, Greenwald S, Ali SY (1992) Calcium phosphate crystal distribution in the superficial zone of human femoral head articular cartilage. *J Anat* **181**, 293–300.

Scotchford CA, Ali SY (1995) Magnesium whitlockite deposition in articular cartilage, a study of 80 specimens from 70 patients. *Ann Rheum Dis* **54**, 339–344.

Scotchford CA, Vickers M, Ali SY (1995) The isolation and characterization of magnesium whitlockite crystals from human articular cartilage. *Osteoarthritis Cartilage* **3**, 79–94.

Stockwell RA (1990) Distribution of crystals in the superficial zone of elderly human articular cartilage of the femoral head in subcapital fracture. *Ann Rheum Dis* **49**, 231–235.

Taylor TKF, Little K (1963) Calcification in the intervertebral disc. *Nature* **208**, 384.

Taylor TK, Ghosh P, Bushell GR, Stephens RW (1980) The scientific basis of the treatment of intervertebral disc disorders. In *Scientific Foundations of Orthopaedics and Traumatology* (eds Owen R, Goodfellow J, Bullough P), pp. 387–406. London: Heinemann Medical.